

DESIGN, SIZING AND SIMULATION OF A HYBRID AC-DC MICROGRID FOR IMPROVING ENERGY EFFICIENCY IN RESIDENTIAL APPLICATIONS

Dante Inga Narváez¹, Tatiane Silva Costa¹, Hugo Soeiro Moreira¹, Marcelo Gradella Villalva¹, Fredrik Wallin²

¹School of Electrical and Computer Engineering, University of Campinas, Brazil.

²Department of Energy, Buildings and Environment, Malardalen University, Sweden.

ABSTRACT

Renewable energy resources have been integrated to the electricity generation industry. Those systems usually require the addition of energy storage units, so microgrids have been proposed to simplify analysis of such complex energy systems. Hybrid AC-DC microgrids use both AC and DC buses in order to reduce power conversion losses due to the AC and DC nature of house loads, so residential buildings became an interesting application field. A hybrid AC-DC microgrid composed of a PV generator, two storage units, AC and DC loads is proposed, which also can connect with the main grid. Power and control subsystems for the converters of the microgrid are described, then load and PV profiles are employed to size generating and storage units of the microgrid. Besides that, simulations under maximum generation and demand events are analyzed, as well as improvement in power efficiency when compared to a traditional AC microgrid.

Keywords: control systems, energy efficiency, power converters, renewable energy resources, storage units.

NONMENCLATURE

Abbreviations

RER	Renewable Energy Resources
PWM	Pulse Width Modulation

Symbols

h	Hour of the day
---	-----------------

1. INTRODUCTION

In last decades, world energy demand has been increasing while fossil fuel reserves have been decreasing through years. Therefore, renewable energy resources (RERs) have become a common topic in academic and industrial fields, in which solar photovoltaic (PV) stands nowadays as one of the most employed renewable resources.

However, RER-based generators show some drawbacks such as intermittent and non predictable availability. Thus, other energy resources and storage systems are usually integrated with them in order to meet user's power and energy demand.

The concept of microgrid was proposed with the aim of simplifying the analysis, monitoring and control of energy systems with several generators, loads and storage devices. Moreover, a hybrid AC-DC microgrid aims increasing energy efficiency by connecting the devices in their corresponding AC or DC buses [1-8].

In this work, a hybrid AC-DC microgrid for residential applications is proposed, which is composed by one photovoltaic generator, two storage units and one interface converter (also distributed loads and connection with the main grid). The studied system is then designed, sized and simulated.

2. DESCRIPTION OF THE SYSTEM

Block diagram of the studied microgrid is shown in Fig 1. Four components are connected to the DC bus: DC load (Ddc), DC battery bank (Sbd) through a DC/DC converter, PV array (Gpd) through another DC/DC converter, and a DC/AC interface converter (Sin). On the other hand, four components can be connected to the AC bus: main grid (Sga), AC load (Dac), AC battery bank (Sba) through a two stage DC/AC converter, and the

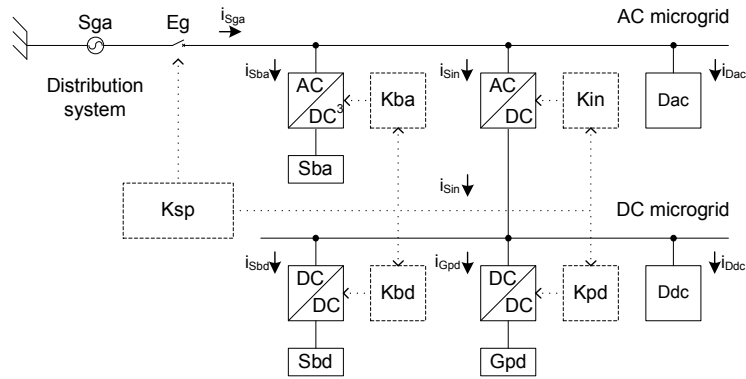


Fig 1 Block diagram of the hybrid AC/DC microgrid

interface converter. Besides that, each one of the four power converters has a control subsystem.

2.1 Power subsystems

Power stages are bidirectional and composed by DC/DC and DC/AC converters [9], the first is shown in Fig 2. DC/DC converter can operate as buck or boost converter. It uses two IGBTs with built-in diodes, one DC inductor (L_d) for current filtering and two capacitors (C_l and C_h) for low-side and high-side voltage filtering.

DC/AC converter can operate as inverter or rectifier,

so it has a DC side and an AC side, see Fig 3. DC/AC converter uses four IGBTs with built-in diodes, one AC inductor (L_a) and two capacitors (C_a and C_d) for AC-side and DC-side voltage filtering.

2.2 Control subsystems

A generic control scheme for the power converters of the hybrid AC-DC microgrid is shown in Fig 4. In case of current control, current reference (i_r) is compared to measured current (i_s) so the error signal is compensated by a current controller (H_{ci}) and applied

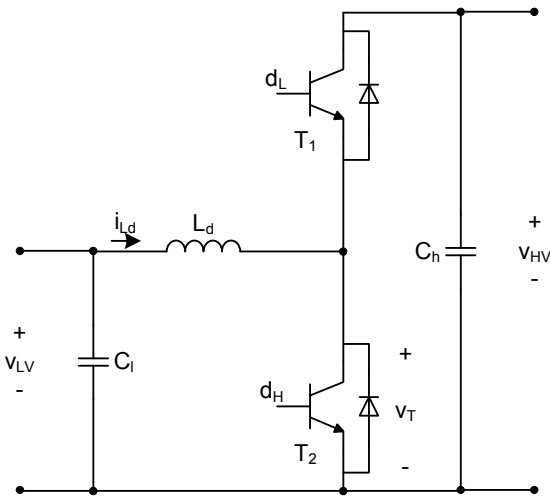


Fig 2 DC/DC power converter

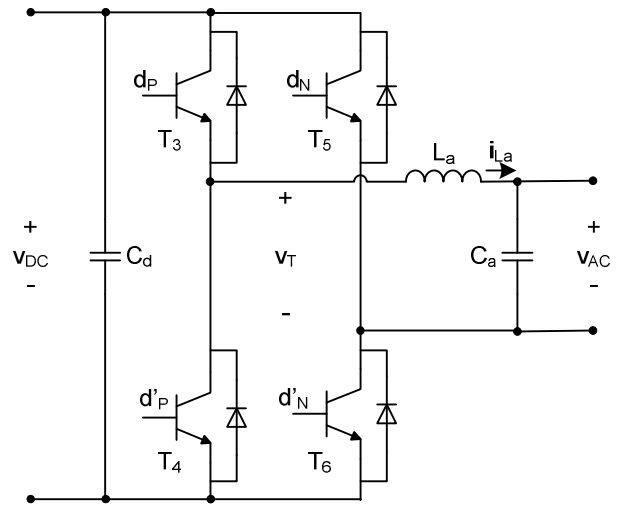


Fig 3 DC/AC power converter

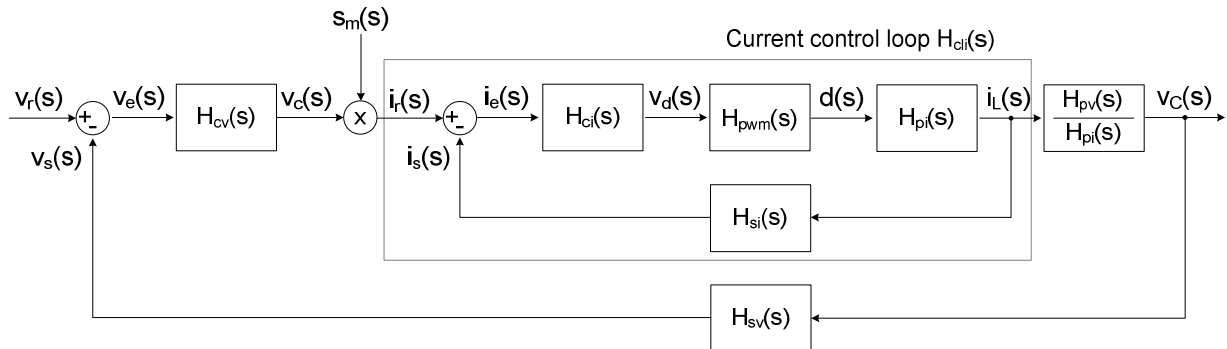


Fig 4 Block diagram of voltage and current controllers for the converters

to the converter current model (H_{pi}) through a Pulse Width Modulation (PWM) block.

Voltage control is implemented by using a double-loop scheme, so the output of the voltage controller (H_{cv}) is treated as current reference, previously multiplied by a sinusoidal signal (S_m) in case of DC voltage control of a DC/AC converter in rectifier mode.

2.3 Modeling of the system

Average theory is used to model dependence of inductor current and capacitor voltage on duty cycle, which is used to control output of the converters [9].

As an example, inductor-current and capacitor-voltage to duty-cycle transfer functions are calculated for a DC/DC converter in buck mode:

$$H_{pi}(s) = \frac{i_{Ld}(s)}{d_L(s)} = \frac{-V_{dc}}{L_d} \times \frac{s + \frac{1}{R_b C_l}}{s^2 + \frac{1}{R_b C_l} s + \frac{1}{L_d C_l}} \quad (1)$$

$$H_{pv}(s) = \frac{v_{Cl}(s)}{d_L(s)} = \frac{V_{dc}}{L_d C_l} \times \frac{1}{s^2 + \frac{1}{R_b C_l} s + \frac{1}{L_d C_l}} \quad (2)$$

In which:

i_{Ld} is the DC-inductor current

v_{Cl} is the low-side-capacitor voltage

d_L is the low-side-transistor control signal

2.4 Design of the controllers

Classical controllers such as PI, Venable compensators, resonant PI and multi-resonant PI are designed by using the phase margin method [10, 11]. Selected controllers for each operating mode of the converters are resumed in Tab 1.

Tab 1 Controllers for the power converters

Converter	Current control	Voltage control
Buck for battery	Type-2	---
Boost converter	Type-3	PI
Inverter islanded	PI	MR-PI
Rectifier	R-PI	PI
Buck for PV array	---	PI
Inverter connected	PI	---

Current controller for the DC/DC converter in buck mode is calculated as an example. If a type-2 Venable compensator [3] is selected as current controller:

$$H_{ci}(s) = A_{ci} \times \frac{s + \frac{w_{ci}}{k_{2i}}}{s(s + w_{ci} k_{2i})} \quad (3)$$

$$\angle H_{li}(jw_{ci}) = -\pi + \varphi_{mi} \Rightarrow k_{2i} = \tan\left(\frac{\varphi_{mi}}{2} - \frac{P_{pi}}{2}\right) \quad (4)$$

$$|H_{li}(jw_{ci})| = 1 \Rightarrow A_{ci} = \frac{w_{ci} k_{2i}}{G_{pi} H_{pwm} H_{si}} \quad (5)$$

In which:

w_{ci} is the crossover angular frequency

φ_{mi} is the current-control-loop phase margin

$P_{pi} = \angle H_{pi}(jw_{ci})$ is the current-model phase at w_{ci}

$G_{pi} = |H_{pi}(jw_{ci})|$ is the current-model gain at w_{ci}

3. SIZING OF THE SYSTEM

First step on designing a hybrid AC-DC microgrid involves sizing generating and storage units according to the average power and energy consumption.

3.1 Load profile

Nominal power and utilization times for several loads for a typical residential building in Brazil are considered to obtain a load active power profile [12], as it is shown in Fig 5. Therefore, storage units should be capable of supplying load maximum power $P_o = 4.8$ kW and daily consumed energy $E_{D(\text{day})}$.

$$E_{D(\text{year})} = 365 \times E_{D(\text{day})} \quad (6)$$

Some DC loads such as TVs, computers and LED lamps could be connected directly to the DC bus of the microgrid, so power demand is divided in this work: 90% power for AC bus and 10% power for DC bus. Therefore: $P_{dac} = 4.5$ kW and $P_{ddc} = 0.5$ kW.

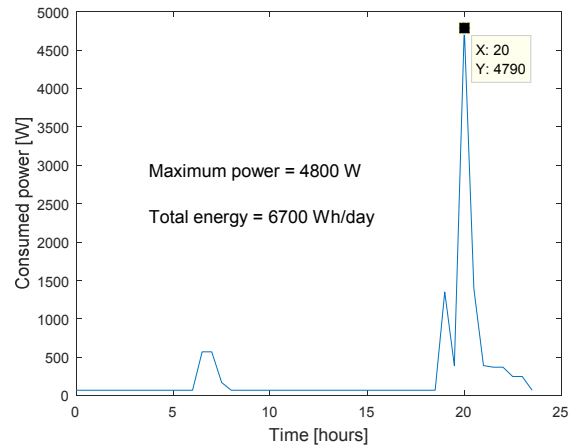


Fig 5 Load profile of a residential building

3.2 Generating unit

Energy produced by a single PV module installed on the horizontal plane is a function of solar irradiation E_s on geographical site (1905 kWh/m²/year for Campinas, Brazil), module area A_M and efficiency η_M [13]:

$$E_{M(\text{year})} = E_{S(\text{year})} \times A_M \times \eta_M \quad (7)$$

By selecting a PV module with peak power $P_M = 240$ W, $A_M = 1.64$ m² and $\eta_M = 14.6\%$, number of PV

modules needed to supply all the consumed energy can be calculated by considering a corrector factor $K_c = 1.2$:

$$N_M = K_c \times E_{D(year)} / E_{M(year)} \quad (8)$$

Besides that, nominal power of PV generating unit $P_{PV} = P_M \times N_M$ is obtained. Then, $N_M = 5$ and $P_{PV} = 1.2 \text{ kW}$. Furthermore, number of PV modules connected in series and parallel depends on maximum DC voltage and current of selected inverter.

3.3 Storage units

Output power of storage units in islanded mode has to match load maximum power, so $P_{BA} = 5 \text{ kW}$. On the other hand, storage energy capability is a function of the energy demand E_D , autonomy in days (N_A) and discharge depth B_D of the batteries:

$$E_A = E_D \times N_A / B_D \quad (9)$$

Thus, battery bank capacity can be obtained [4] (number of batteries connected in series and parallel depends on that value and selected battery):

$$C_{BB} = E_A / V_{BB} \quad (10)$$

4. SIMULATION RESULTS

Hybrid AC-DC microgrid was designed and simulated under several scenarios. According to load profile shown in Fig 5, analysis at maximum demand time (about 8pm) and when the PV generator produces maximum power (about midday) are of interest. Component values, voltage, frequency and power levels are shown in Tab 2.

Tab 2 Components of the studied microgrid

Parameter	Value	Parameter	Value
V_b	240 V	$V_{AC(rms)}$	220 V
R_b	1.2Ω	f_g	60 Hz
$C_{l,a}$	10 μF	R_g	0.1Ω
$L_{d,a}$	10 mH	L_g	1 mH
$C_{h,d}$	1 mF	$P_{AC-load}$	4.5 kW
V_{DC}	450 V	$P_{DC-load}$	0.5 kW
V_{PV}	240 V	P_{PV}	1.2 kW

4.1 Simulation at maximum PV generation

In grid-connected mode, storage units are maintained in full charge by consuming a small percentage of their nominal input current. Current waveforms when the microgrid is connected to the main grid and the PV generator (Gpd) is at maximum power (around midday) are shown in Fig 6. In this case, main grid (Sga) controls AC bus voltage and frequency,

thus the interface converter injects power (1.4 kW) from the DC bus to the AC bus, which is enough to supply the AC load (90 W) and export power to the main grid (1.3 kW). On the other hand, DC battery converter (Sbd) controls the DC bus voltage, so the PV unit can supply 1.2 kW, while Sbd supplies 200 W and Ddc consumes 10 W.

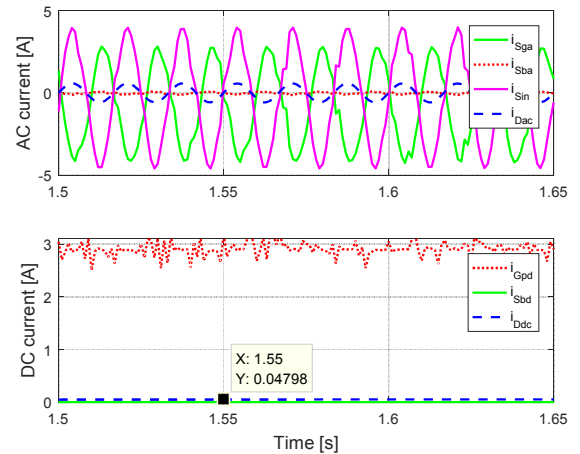


Fig 6 Currents at peak PV generation.

4.2 Simulation at maximum load demand

AC and DC current waveforms when the microgrid is connected to the main grid and the load demand is high (around 8pm) can be shown in Fig 7. DC bus voltage is controlled by the interface converter (Sin), then DC load (Ddc) consumes 500 W, DC battery (Sbd) consumes 100 W (to maintain the battery bank in full-charge state) and PV generator (Gpd) does not produce power. In contrast, AC bus voltage and frequency are controlled by the main grid (Sga), so AC load consumes 4.5 kW, AC battery consumes 10 W and the main grid supplies 5.1 kW. It can be noticed that the interface converter transfers 600 W from the DC bus to the AC bus.

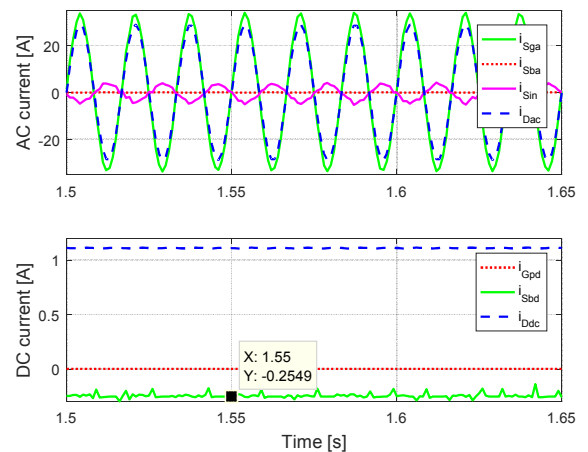


Fig 7 Currents at peak load demand.

4.3 Efficiency analysis

Considering that power converters have a conversion efficiency of about 95%, decrease in converting power losses can be estimated when comparing the hybrid AC-DC microgrid with a traditional AC microgrid. Results are shown in Tab 3. It can be noticed that DC loads do not need AC/DC conversion in a hybrid AC/DC microgrid, so it represents difference in power losses. Therefore, critical hours are analyzed: midday and 8pm. For the hybrid AC-DC microgrid, 2.82 kW is transferred by the power converters. For the traditional AC microgrid, DC loads will require an additional AC/DC conversion, which means more power losses. Thus, it can be seen that power losses with hybrid AC-DC microgrid are less than losses with a traditional AC microgrid.

Tab 3 Losses comparison for hybrid and AC microgrids

System\Hour	Midday	8pm
$S_{ba}, S_{in}, S_{bd}, G_{pd}$	5%(2.82 kW)	5%(1.22 kW)
D_{dc}	0%(10 W)	0%(0.5 kW)
AC-DC ugrid	141 W	61 W
$S_{ba}, S_{in}, S_{bd}, G_{pd}$	5%(2.82 kW)	5%(1.22 kW)
D_{dc}	5%(10 W)	5%(0.5 kW)
AC ugrid	141.5 W	86 W

5. CONCLUSIONS

A procedure to design rated powers of components of a hybrid AC-DC microgrid is discussed in this work. For residential applications, load demand defines size of power generators, while autonomy time determines size of the storage units.

Average modeling and classical controllers are used to verify stable operation of the AC-DC microgrid under maximum generation and maximum demand events. It is shown that the power converters can be reconfigured according to changes in generation and demand.

Finally, an estimation of power losses when compared to a traditional AC microgrid is developed. It is demonstrated that more DC generators and loads will require more DC/AC converters, so power losses are reduced when using a hybrid AC-DC microgrid with an only DC/AC interface converter.

ACKNOWLEDGEMENT

This work was supported by CNPq, CAPES, FAPESP (2016/08645-9), CPFL (ANEEL/PA3032), and BYD Energy Brazil (MCTIC-PADIS).

REFERENCE

- [1] X. Liu, P. Wang, P. C. Loh. A hybrid ac/dc micro-grid. In Conference Proceedings IPEC, 2010.
- [2] Hossam A. Gabbar, Mohamed El-Hendawi, G. El-Saady, and El-Nobi A. Ibrahim. Supervisory controller for power management of ac/dc microgrid. In IEEE Smart Energy Grid Engineering (SEGE), 2016.
- [3] F. Luo, K. H. Loo, and Y. M. Lai. A hybrid ac/dc microgrid control scheme with voltage-source inverter-controlled interlinking converters. In 18th European Conference on Power Electronics and Applications (EPE'16 ECCE Europe), 2016.
- [4] Pengxiang Xing, Lijun Fu, Gang Wang, Fan Ma, Liang Zhou, and Yi Wang. Control strategy of seamless operation mode switch for ac/dc hybrid microgrid. In IEEE International Conference on Aircraft Utility Systems (AUS), 2016.
- [5] B. Zhao, Q. Song, and W. Liu. A practical solution of high-frequency-link bidirectional solid-state transformer based on advanced components in hybrid microgrid. IEEE Transactions on Industrial Electronics,, 2015.
- [6] J. He, Y. W. Li, C. Wang, Y. Pan, C. Zhang, and X. Xing. A hybrid microgrid with parallel and series connected micro-converters. IEEE Transactions on Power Electronics, 2017.
- [7] N. Korada and M. K. Mishra. Grid adaptive power management strategy for an integrated microgrid with hybrid energy storage. IEEE Transactions on Industrial Electronics, 2017.
- [8] S. Kotra and M. K. Mishra. A supervisory power management system for a hybrid microgrid with hess. IEEE Transactions on Industrial Electronics, 2017.
- [9] R.W. Erickson, D. Maksimovic, Fundamentals of Power Electronics, 2nd edn., Springer Press, 2001.
- [10] H.D. Venable, The k Factor: A New Mathematical Tool for Stability Analysis and Synthesis, 1983, pp. 1–10.
- [11] D. I. Narvaez, M. V. G. Reis, T. A. S. Barros, E. Ruppert, and M. G. Villalva. Performance comparison of dc and ac controllers for a two- stage power converter in energy storage application. Electric Power Systems Research, 2018.
- [12] Diretoria de Comunicação Empresarial e Relações Institucionais. Cartilha de utilização consciente de energia elétrica. CPFL Brazil, 2017. (In Portuguese)
- [13] M. G. Villalva, Energia Solar Fotovoltaica: Conceitos e aplicações, Erica, 2012. (In Portuguese)